Stanford Exploration Project, Report 102, October 25, 1999, pages 143–157

Estimating rock porosity and fluid saturation using only seismic velocities

James G. Berryman,[1] *Patricia A. Berge,*[2] *and Brian P. Bonner*[3]

keywords: *poroelasticity, seismic waves, patchy saturation, porosity estimation*

ABSTRACT

Evaluation of the fluid content in deep earth reservoirs or of fluid contaminants in shallow earth environments has required the use of geophysical imaging methods such as seismic reflection prospecting. The processing of these seismic data has involved meticulous care in determining the changes in reflected seismic amplitude as the point of observation for the received signals at the earth's surface is moved away from the seismic source (Ostrander, 1984). The now commonly used method called AVO (for Amplitude Versus Offset) is based on theories of fluid-saturated and partially saturated rocks that have been available since the 1950's. Here we present a new synthesis of the same physical concepts that uses some of the same data as AVO (compressional wave velocities) together with some different data (shear wave velocities) in a scheme that is much simpler to understand and apply, yet yields the desired information about porosity and fluid saturation. The method is designed especially for near surface applications and for use with crosswell and VSP data, but it can also be applied to reflection seismic data assuming that reliable interval velocities are available. Since the new method does not require hard-to-obtain wave amplitude information, it can be used for a wider range of seismic source-receiver configurations, including crosswell seismic transmission tomography (well-to-well), vertical seismic profiling (well-to-surface), as well as seismic reflection profiling (surface-to-surface), since reflection data can be used but are not a necessity.

INTRODUCTION

Resolution of various practical and scientific issues in the earth sciences depends on knowledge of fluid properties underground. In environmental cleanup applications, the contaminant to be removed from the earth is often a liquid such as gasoline or oil, or ground water contaminated with traces of harmful chemicals. In commercial oil and gas exploration, the fluids of interest are hydrocarbons in liquid or gaseous form. In analysis of the earth structure, partially

[1]**email**: berryman@sep.stanford.edu
[2]Lawrence Livermore National Lab, P. O. Box 808, L-201, Livermore, CA 94550
email: berge1@llnl.gov
[3]Lawrence Livermore National Lab, P. O. Box 808, L-201, Livermore, CA 94550
email: bonner1@llnl.gov

melted rock is key to determining temperature and local changes of structure in the earth's mantle. In all cases the tool commonly used to analyze the fluid content is measurements of seismic (compressional and shear) wave velocities in the earth. Depending on the application, the sources of these waves may be naturally occurring such as earthquakes, or man-made such as reflection seismic surveys at the surface of the earth, vertical seismic profiling, or still more direct measurements using logging tools in either shallow or deep boreholes.

Underground fluids occupy voids between and among the solid earth grains. When liquid or gas completely fills interconnnecting voids, a well-known result due to Gassmann (1951) predicts how the composite elastic constants that determine seismic velocities should depend on the fluid and drained rock or soil elastic constants and densities [also see tutorial by Berryman (1999)]. The formulas due to Gassmann are low frequency (seismic) results and both laboratory and well-log measurements of wave velocities have been observed to deviate markedly from Gassmann's predictions at higher (sonic and ultrasonic) frequencies. This is especially so for partial saturation conditions (*i.e.*, when the fluid in each pore is a mixture of gas and liquid). In some cases these deviations can be attributed (Berryman *et al.*, 1988; Endres and Knight, 1989; Mavko and Nolen-Hoeksema, 1994; Dvorkin and Nur, 1998) to "patchy saturation," meaning that some void regions are fully saturated with liquid and others are filled with gas. When the concept of patchy saturation is applicable, Gassmann's formulas apply locally (but not globally) and must be averaged over the volume to obtain the overall seismic velocity of the system. In other cases, neither Gassmann's formulas nor the "patchy saturation" model seem to apply to seismic data. In these cases a variety of possible reasons for the observed velocity discrepancies have been put forward, including viscoelastic effects (velocity decrement due to frequency-dependent attenuation), fluid-enhanced softening of intragranular cementing materials, chemical changes in wet clays that alter mechanical properties, etc.

The objective of the present study therefore has been to find a method of using seismic data to estimate porosity and saturation, regardless of whether the rock or soil fits the Gassmann, the patchy saturation, or some other model. Seismic data typically provide two measured parameters, v_p and v_s (compressional and shear wave velocities, respectively). Simple algebraic expressions relate v_p and v_s to the Lamé parameters λ and μ of elasticity theory, and the overall density ρ. These relationships are well-known (Ewing *et al.*, 1957; Aki and Richards, 1980), but the parameter λ is seldom used to analyze seismic data. Our first new way of displaying seismic data is to plot data points in the $(\rho/\mu, \lambda/\mu)$-plane — instead of (for example) the (v_p, v_s)-plane. (Note that $\rho/\mu = 1/v_s^2$.) The advantage of this plot is that, when the liquid and gas are either mixed homogeneously throughout (Gassmann's assumption) or are fully segregated throughout (patchy saturation), most of the data will fall along one or the other of two straight lines. Significant deviations from these two expected behaviors then provide a clear indication that the data violate some of the assumptions in Gassmann's simple model, and furthermore provide clues to help determine which assumptions are being violated. Our second innovation in displaying seismic data is to plot the data points in the $(\rho/\lambda, \mu/\lambda)$-plane. This second approach involves the use of an easily understood mathematical trick that leads naturally to universal and easily interpreted behavior; virtually all laboratory data on partial saturation for similar rocks that we have analyzed plot with minimal scatter along straight lines in this plane. The length and slope of these lines have quantitative predictive capabilities for measurements of both partial saturation and porosity. We have used sonic and ultrasonic

laboratory data in the present study, but the results provide very strong indications that equally useful relationships among seismic parameters, porosity, and saturation will be obtained from seismic data collected at lower frequencies in the field.

BASICS OF ELASTIC WAVE PROPAGATION

For isotropic elastic materials there are two bulk elastic wave speeds (Ewing *et al.*, 1957; Aki and Richards, 1980), compressional $v_p = \sqrt{(\lambda + 2\mu)/\rho}$ and shear $v_s = \sqrt{\mu/\rho}$. Here the Lamé parameters λ and μ are the constants that appear in Hooke's law relating stress to strain in an isotropic material. The constant μ gives the dependence of shear stress on shear strain in the same direction. The constant λ gives the dependence of compressional or tensional stress on extensional or dilatational strains in orthogonal directions. For a porous system with porosity ϕ (void volume fraction) in the range $0 < \phi < 1$, the overall density of the rock or sediment is just the volume weighted density given by $\rho = (1-\phi)\rho_s + \phi[S\rho_l + (1-S)\rho_g]$, where ρ_s, ρ_l, ρ_g are the densities of the constituent solid, liquid and gas, respectively, and S is the liquid saturation, *i.e.* the fraction of liquid-filled void space in the range $0 \leq S \leq 1$ (Domenico, 1974). When liquid and gas are distributed uniformly in all pores and cracks, Gassmann's equations say that, for quasistatic isotropic elasticity and low frequency wave propagation, the shear modulus μ will be mechanically independent of the properties of any fluids present in the pores, while the overall bulk modulus $K \equiv \lambda + \frac{2}{3}\mu$ of the rock or sediment including the fluid depends in a known way on porosity and elastic properties of the fluid and dry rock or sediment (Gassmann, 1951). Thus, in the Gassmann model, the Lamé parameter λ is elastically *dependent* on fluid properties, while μ is not. The density ρ also depends on saturation. At low liquid saturations, the fluid bulk modulus is dominated by the gas, and therefore the effect of the liquid on λ is negligible until full saturation is approached. This means that both seismic velocities v_p and v_s will decrease with increasing fluid saturation (Domenico, 1974; Wyllie *et al.*, 1956; Wyllie *et al.*, 1958) due to the "density effect," *i.e.*, the only quantity changing is the density which increases in the denominators of both v_p^2 and v_s^2. As full saturation is approached, the shear velocity continues its downward trend, while the compressional velocity suddenly (over a very narrow range of change of saturation) shoots up to its full saturation value. An example (Murphy, 1982; 1984) of this behavior is shown in Figure 1a. This is the expected (ideal Gassmann) behavior of porous rocks at low frequencies (sonic and below).

PREDICTIONS OF THE THEORY

Gassmann's equation (Gassmann, 1951) for fluid substitution states that

$$K = K_{dr} + \frac{\alpha^2}{(\alpha - \phi)/K_m + \phi/K_f}, \tag{1}$$

where K_m is the bulk modulus of the solid mineral, K_{dr} is the bulk modulus of the drained porous frame, $\alpha = 1 - K_{dr}/K_m$ is the Biot-Willis (1957) parameter, ϕ is the porosity, and K

is the effective bulk modulus of the undrained fluid-mixture-saturated porous medium, where, for partial saturation conditions with homogeneous mixing of liquid and gas,

$$1/K_f = S_l/K_l + (1-S_l)/K_g. \tag{2}$$

The saturation level of liquid is S_l, K_l is the bulk modulus of the liquid, and K_g is the bulk modulus of the gas. When S_l is small, (2) shows that $K_f \simeq K_g$, since $K_g \ll K_l$. As $S_l \to 1$, K_f remains close to K_g until S_l closely approaches unity. Then, K_f changes rapidly (over a small range of saturations) from K_g to K_l.

The bulk modulus K_f contains the only dependence on S_l in (1). Thus, for porous materials satisfying Gassmann's homogeneous fluid conditions and for low enough frequencies, the theory predicts that, if we use seismic velocity data in a two-dimensional plot with one axis being the saturation S_l and the other being the ratio $\lambda/\mu = (v_p/v_s)^2 - 2$, then the results will lie along a straight (horizontal) line until the saturation reaches $S_l \simeq 1$ (around 95% or higher), where the curve formed by the data will quickly rise to the value determined by the velocities at full liquid saturation.

On the other hand, if the porous medium contains gas and liquid mixed in a heterogeneous manner, so that patches of the medium hold only gas while other patches hold only liquid, then the theory predicts that, depending to some extent on the spatial distribution of the patches, the results will deviate from Gassmann's results. If we consider the most extreme cases of spatial distribution possible, which are laminated regions of alternating liquid saturation and gas saturation, then the effective bulk modulus at low frequencies will be determined by an average of the two extreme values of (1): $K(S_l = 0) = K_{dr}$ and $K(S_l = 1)$. Using saturation as the weighting factor, the harmonic mean and the mean are the well-known results for these two extremes of behavior. Of these two, the one that differs most from (1) is the mean. But, on our plot, the results for the mean will again lie along a straight line, So this time the line goes directly from the dry (or unsaturated $S_l = 0$) value to the fully saturated value ($S_l = 1$). The two straight lines described are rigorous results of the theory, and form two sides of a triangle that will contain all data for partially saturated systems, regardless of the type of saturation present.

FIRST NEW METHOD OF DATA DISPLAY

In order to separate effects of liquids on Lamé's parameter λ from well-understood effects of liquids on the density ρ, while taking full advantage of the fluid-effect independence of shear modulus μ, we will now combine the v_p and v_s data into a new type of plot. To take advantage of the predictions of the theory described above, we will plot seismic velocity data in a two-dimensional array with one axis being $\rho/\mu = 1/v_s^2$ and the other being the ratio $\lambda/\mu = (v_p/v_s)^2 - 2$. Now, the ratio $\rho/\mu = 1/v_s^2$ acts as a proxy for S which we do not know, but both S and ρ/μ are simply linear functions of S in the region of low frequencies being considered. For porous materials that satisfy Gassmann's homogeneous fluid condition the result should be a straight (horizontal) line until the saturation reaches $S \simeq 1$ (around 95% or higher), where the data should quickly rise to a value determined by the velocities

at full liquid saturation. This behavior is observed in Figure 1b. Note that, although this behavior is qualitatively similar to that of v_p in Figure 1a, we are now using only the seismic velocities themselves (no saturation data are required to generate this plot, although in this case saturation can be inferred at least qualitatively). The behavior we observe here is traditional Gassmann-Domenico predictions (Domenico, 1974) for partial saturation.

If all the other assumptions of the Gassmann model are satisfied, but the liquid and gas are not distributed uniformly (so that different pores have different saturation levels), then we have the circumstances that may better fit the "patchy saturation" model (Berryman *et al.*, 1988; Endres and Knight, 1989; Mavko and Nolen-Hoeksema, 1994; Dvorkin and Nur, 1998). In that case, for the plot of λ/μ vs. ρ/μ, instead of data following a horizontal line with a jump up at the high saturation end (*e.g.*, Figure 1b), the ideal patchy saturation model (for completely segregated liquid and gas pockets) would predict that the data should lie on another straight line connecting to the two end points (dry and saturated) on this plot. These straight lines have been superimposed on the plots [obtained using data from Murphy (1982; 1984) and from Knight and Nolen-Hoeksema (1990)] for Figures 1b, 1d, and 1f. The anticipated behavior has been observed in Figure 1b and in other data not shown here, but two distinctly different types of behavior are observed in Figures 1d and 1f.

Plots of velocity versus saturation and of λ/μ versus ρ/μ for two sandstones that apparently do not behave according to Gassmann's model are shown in Figures 1c-1f. These apparent deviations from the range of expected behaviors (from purely homogeneous mixed fluids to purely segregated patchy saturation) are resolved by including another display for these three sandstones (Murphy, 1982; 1984; Knight and Nolen-Hoeksema, 1990) in Figures 2a,c,e and corresponding plots for three limestones (Cadoret, 1993; Cadoret *et al.*, 1995; Cadoret *et al.*, 1998) in Figures 2b,d,f. Now the ratio λ/μ is plotted versus *saturation* measured in the laboratory, and we observe in all these cases that the basic plot structures we had anticipated for Figures 1b, 1d, and 1f are in fact confirmed. What we learn from this observation is that the quantity ρ/μ, which we wanted to use as a proxy for the saturation S, is *not* always a good proxy at high frequencies. We can safely attribute the discrepancies in Figures 1d and 1f to effects of high frequency dispersion as predicted by Biot's theory (Biot, 1956a; 1956b; 1962). Even the seemingly odd negative slope of the patchy saturation lines in Figure 1f can be understood as a predicted high frequency effect on the shear velocity (Berryman, 1981).

This first new plotting method is limited by the implicit assumptions that the shear modulus is independent of the presence of fluids and that frequency dispersion for shear velocity is negligible. The assumption that the materials' shear properties are independent of the fluid is based on theoretical predictions about mechanical behavior only, and any chemical interactions between fluid and rock that might soften grain contacts could easily account for some of these discrepancies. Fluid-induced swelling of either interstitial or intergranular clays is another possible source of discrepancy as are fluid-induced pressure effects if the fluid is overpressured and therefore tending to severely weaken the rock. All of the chemical effects mentioned should become active with even very small amounts of fluid present, but probably do not have very significant frequency dependence (at least within the seismic frequency band). On the other hand, we must also take into account Biot's theory (Biot, 1956a; 1956b; 1962) of acoustics in porous media, which generalizes Gassmann's theory to higher frequencies and has

been shown to be a very reliable predictor of behavior in simple porous systems (Berryman, 1995). There are frequency dependent (dispersion) effects predicted by Biot's theory that can lead to complications difficult to resolve with the severely frequency-band limited data that are normally available.

Fortunately, Cadoret and colleagues (Cadoret, 1993; Cadoret *et al.*, 1995; Cadoret *et al.*, 1998) have in recent years performed a very extensive series of tests on limestones, including both ultrasonic and sonic experiments and with different means of achieving various levels of partial saturation. Figure 3b shows results obtained for an Estaillades limestone at 500 kHz. This material behaves very much like the sandstones we have already considered here, and appears to obey the Gassmann predictions very well all the way up to the ultrasonic frequency regime. There were several other limestones that were found to have similar if not quite such good behavior. On the other hand, there were two limestone samples (a granular Lavoux limestone and an Espeil limestone) that were found to have very strong dispersion in the ultrasonic frequency band. These materials do not behave as expected when the data are plotted as in either Figure 1 or Figure 2. However, since extensional wave and shear wave data (Cadoret, 1993; Cadoret *et al.*, 1995; Cadoret *et al.*, 1998) at 1 kHz were also collected for these same samples, we have computed the necessary quantities using standard formulas and plotted them for these two materials in Figures 2d and 2f. We see that even for these two badly behaved materials (in the ultrasonic band) the plots at lower frequency become easy to interpret again. These results provide a very strong indication that plots such as those in Figure 1 will be readily interpreted for all porous materials at seismic frequencies.

ANOTHER NEW METHOD OF DATA DISPLAY

By making two seemingly small changes in the method of display, we now arrive at one of the main points of this paper. Since the expected behavior for Gassmann materials as observed in Figure 1b is a horizontal straight line for most values of saturation (*i.e.*, λ/μ is expected to be almost constant until high saturation levels are reached), it is natural to consider dividing ρ/μ by λ/μ, and then plotting the points again in the $(\rho/\lambda,\ \mu/\lambda)$-plane. In the straight-line portion of the curve from Figure 1b, the only effect will be a change of scale, but large changes will result in the points representing full saturation or nearly full saturation. The results of this new plotting method are displayed in Figure 3. We observe that in all cases the result is apparently a straight line. This linear behavior is expected for a Gassmann material, since λ is just a scaling factor, μ is unaffected by saturation, and ρ is linearly dependent on saturation. It would also be expected for a non-Gassmann material in which the effect of fluids on λ was negligible compared to the effect on μ. It may also be expected for the case of patchy saturation if chemical interactions cause μ to change with saturation, because then μ for the porous medium would be some weighted average of μ for the dry case and μ for the fully saturated, chemically altered portions of the rock.

Figure 3a shows the same sandstone data as Figure 1. Similar data for five limestone samples (Cadoret, 1993; Cadoret *et al.*, 1995; Cadoret *et al.*, 1998) are plotted in Figure 3b. The straight line correlation of the data in this display is clearly confirmed by the limestone data. Numerous other examples of the correlation have been observed. No examples of appropriate

data for partially saturated samples with major deviations from this behavior have been observed, although an extensive survey of available data sets has been performed for materials including limestones, sandstones, granites, unconsolidated sands, and some artificial materials such as ceramics and glass beads. This straight line correlation is a very robust feature of partial saturation data. The mathematical trick that brings about this behavior will be explained in simple terms below following a brief discussion of the usefulness of this display.

We now have two new methods of data display, both using the Lamé parameter λ in a critical role. We therefore call this pair of plotting methods the "λ-diagrams."

POROSITY CORRELATION

An additional feature of displays of the type presented in Figure 3 is that the slopes of the straight lines, at least for samples of similar material character, are inversely correlated with the porosity of the samples. This observation is highlighted in Figures 3c and 3d. Figure 3c shows results from a series of fused glass-bead samples (Berge *et al.*, 1995) of uniform composition that was fabricated, with lower porosities being achieved by varying temperatures and length of sintering times. The porosities are distributed almost perfectly in Figure 3c, with the lower porosity lines having higher slopes and higher porosity lines having lower slopes. The experimental error in the stated porosity measurements $\simeq \pm 0.6\%$, so that the main discrepancy observed here with misalignment between the samples at $\phi = 36.0\%$ and $\phi = 36.5\%$ suggests that this display may provide a more sensitive means of determining the porosity. Figure 3d shows similar behavior for very low porosity granite (Nur and Simmons, 1969), having $\phi \simeq 1\%$; as the pressure is increased, the porosity in the material is steadily decreased mostly due to crack closure.

WHY THE SECOND DISPLAY IS ALWAYS APPROXIMATELY LINEAR

We can understand both the linearity and the apparent dependence of the data correlation on porosity in the second plotting method shown in Figure 3 by understanding some simple facts about such displays. Consider a random variable X. If we display data on a plot of either X vs. X or $1/X$ vs. $1/X$, the result will always be a perfect straight line. In both cases the slope of the straight line is exactly unity and the intercept of the line is the origin of the plot (0, 0). Now, if we have another variable Y and plot Y/X vs. $1/X$, then we need to consider two pertinent cases: (1) If $Y = constant$, then the plot of Y/X vs. X will again be a straight line and the intercept will again be the origin, but the slope will be Y, rather than unity. (2) If $Y \neq constant$ but is a variable with small overall variation (small dynamic range), then the plot of Y/X vs. $1/X$ will not generally be exactly a straight line. The slope will be given approximately by the average value of Y and the intercept will be near the origin, but its precise value will depend on the correlation (if any) of Y and X. In our second method of plotting, the variable λ/ρ plays the role of X and the variable $v_s^2 = \mu/\rho$ plays the role of Y. The plots are approximately linear because this method of display puts the most highly variable combination of constants λ/ρ in the role of X, and the least variable combination of constants v_s^2 in the role of Y. Furthermore,

the slope of the observed lines is therefore correlated inversely with the porosity ϕ because the slope is approximately the average value of v_s^2 which is well-known to decrease monotonically with increasing porosity.

ON UNIQUENESS OF λ-DIAGRAMS

Since the possible linear combinations of the elastic bulk and shear moduli (K and μ) is infinite, it is natural to ask why (or if) $\lambda = K - \frac{2}{3}\mu$ is special? Is there perhaps some other combination of these constants that works as well or even better than the choice made here? There are some rather esoteric reasons based on recent work (Berryman *et al.*, 1999) in the analysis of layered anisotropic elastic media that lead us to believe that the choice λ is indeed special, but we will not try to describe these reasons here. Instead we will point out some general features of the two types of plots that make it clear that this choice is generally good, even though others might be equally good or even better in special circumstances. First, in the diagram using the (ρ/μ, λ/μ)-plane, it is easy to see that *any* plot of data using linear combinations of the form (ρ/μ, $(\lambda + c\mu)/\mu$), where c is any real constant, will have precisely the same information and the display will be identical except for a translation of the values along the ordinate by the constant value c. Thus, for example taking $c = \frac{2}{3}$, plots of (ρ/μ, K/μ) will have exactly the same interpretational value as those presented here. But if we now reconsider the second type of plot for each of these choices, we need to analyze plots of the form ($\rho/(\lambda + c\mu)$, $\mu/(\lambda + c\mu)$). Is there an optimum choice of the parameter c that makes the plots as straight as possible whenever the only variable is the fluid saturation? It is not hard to see that the class of best choices always lies in the middle of the range of values of λ/μ taken by the data. So setting $-c = \frac{1}{2}(\min(\lambda/\mu) + \max(\lambda/\mu))$ will always guarantee that there are very large positive and negative values of $\mu/(\lambda + c\mu)$, and therefore that these data fall reliably (if somewhat approximately) along a straight line. But the minimum value of λ/μ has an absolute minimum of $-\frac{2}{3}$, based on the physical requirement of positivity of K. So $c < \frac{2}{3}$ is a physical requirement, and since $\max \lambda/\mu \simeq +\frac{2}{3}$ is a fairly typical value for porous rocks, it is expected that an optimum value of $c \leq 0$ will generally be obtained using this criterion. Thus, plots based on bulk modulus K instead of λ will not be as effective in producing the quasi-orthogonality of porosity and saturation that we have obtained in the second style of plotting. We conclude that the choice λ is not unique (some other choices might be as good for special data sets) but it is nevertheless an especially simple choice and also expected to be quite good for most real data.

CONCLUSIONS

The new plotting strategies described in this paper provide promising new methods for estimating both porosity and saturation from seismic data as well as for distinguishing types of fluid saturation present in the earth. The methods will apply to low frequency (seismic) data whether or not they fit Gassmann's model (Gassmann, 1951) or a patchy saturation model (Berryman *et al.*, 1988; Endres and Knight, 1989; Mavko and Nolen-Hoeksema, 1994; Dvorkin and

Nur, 1998). At these low frequencies, the type of saturation present (well-segregated liquids and gases, homogeneous fluid mixtures, or some patchy saturation state intermediate between these two extremes) determines the location of data points on the (ρ/μ, λ/μ)-plane. High frequency (ultrasonic) data are more likely to contain wave attenuation and dispersion effects that complicate our analyses, but as shown here they nevertheless do not seriously affect our interpretations based on Lamé's elastic parameter λ as long as the data are taken in a range of frequencies that avoids the very largest dispersive effects. We find porosity is correlated inversely with the slopes of the data-distribution lines in the (ρ/λ, μ/λ)-plane (see Figure 3). This fact can be used to sort field data into subsets having similar material characteristics and porosities for display on the more sensitive (ρ/μ, λ/μ) plots. The main conclusion associated with Figure 2 is that saturation is an approximately (within normal data scatter) monotonic function of λ/μ (as in Figure 1), and therefore also of μ/λ (as in Figure 3). So saturation can be estimated from knowledge of location along the lines of Figure 3 and relative changes of saturation can be determined with a high level of confidence. After sorting seismic data by material characteristics and porosity using the (ρ/λ, μ/λ)-diagram, the resulting data subsets can then be displayed in the (ρ/μ, λ/μ)-plane and used to infer the local states of saturation.

ACKNOWLEDGMENTS

We thank Bill Murphy and Rosemarie Knight for providing access to their unpublished data files. We thank Norman H. Sleep for his insight clarifying the significance of our second method of plotting seismic data.

REFERENCES

Aki, K., & Richards, P. G., 1980, *Quantitative Seismology: Theory and Methods*, Vols. I & II, W. H. Freeman and Company, New York.

Berge, P. A., Bonner, B. P., & Berryman, J. G., 1995, Ultrasonic velocity-porosity relationships for sandstone analogs made from fused glass beads: *Geophysics* **60**, 108–119.

Berryman, J. G., 1981, Elastic wave propagation in fluid-saturated porous media: *J. Acoust. Soc. Am.* **69**, 416–424.

Berryman, J. G., 1995, Mixture theories for rock properties: *Rock Physics and Phase Relations: A Handbook of Physics Constants*, American Geophysical Union, Washington, D.C., pp. 205–228.

Berryman, J. G., 1999, Origin of Gassmann's equations: *Geophysics* **64**, *in press*; **SEP-102**, October, 1999, pp. 133–137.

Berryman, J. G., Grechka, V. Y. & Berge, P. A., 1999, Analysis of Thomsen parameters for finely layered VTI media: *Geophys. Prospect.* **47**, 959–978; **SEP-94**, pp. 247–261.

Berryman, J. G., Thigpen, L., & Chin, R. C. Y., 1988, Bulk elastic wave propagation in partially saturated porous solids: *J. Acoust. Soc. Am.* **84**, 360–373.

Biot, M. A., 1956a, Theory of propagation of elastic waves in a fluid-saturated porous solid. I. Low-frequency range: *J. Acoust. Soc. Am.* **28**, 168–178.

Biot, M. A., 1956b, Theory of propagation of elastic waves in a fluid-saturated porous solid. II. Higher frequency range: *J. Acoust. Soc. Am.* **28**, 179–1791.

Biot, M. A., 1962, Mechanics of deformation and acoustic propagation in porous media: *J. Appl. Phys.* **33**, 1482–1498.

Biot, M. A., and D. G. Willis, 1957, The elastic coefficients of the theory of consolidation: *J. Appl. Mech.* **24**, 594–601.

Cadoret, T., 1993, *Effet de la saturation eau/gaz sur les propriétés acoustiques des roches. Étude aux fréquences sonores et ultrasonores.* Ph.D. Dissertation, Université de Paris VII, Paris, France.

Cadoret, T., Marion, D., & Zinszner, B., 1995, Influence of frequency and fluid distribution on elastic wave velocities in partially saturated limestones: *J. Geophys. Res.* **100**, 9789–9803.

Cadoret, T., Mavko, G., & Zinszner, B., 1998, Fluid distribution effect on sonic attenuation in partially saturated limestones: *Geophysics* **63**, 154–160.

Domenico, S. N., 1974, Effect of water saturation on seismic reflectivity of sand reservoirs encased in shale: *Geophysics* **39**, 759–769.

Dvorkin, J. & Nur, A., 1998, Acoustic signatures of patchy saturation: *Int. J. Solids Struct.* **35**, 4803–4810.

Endres, A. L., & Knight, R., 1989, The effect of microscopic fluid distribution on elastic wave velocities. *Log Anal.* **30**, 437–444.

Ewing, W. M., Jardetsky, W. S., & Press, F., 1957, *Elastic Waves in Layered Media*, McGraw-Hill, New York.

Gassmann, F., 1951, Über die elastizität poröser medien: *Vierteljahrsschrift der Naturforschenden Gesellschaft in Zürich*, **96**, 1–23.

Knight, R., & Nolen-Hoeksema, R., 1990, A laboratory study of the dependence of elastic wave velocities on pore scale fluid distribution: *Geophys. Res. Lett.* **17**, 1529–1532.

Mavko, G. & Nolen-Hoeksema, R., 1994, Estimating seismic velocities at ultrasonic frequencies in partially saturated rocks: *Geophysics* **59**, 252–258.

Murphy, William F., III, 1982, *Effects of Microstructure and Pore Fluids on the Acoustic Properties of Granular Sedimentary Materials*, Ph.D. Dissertation, Stanford University.

Murphy, William F., III, 1984, Acoustic measures of partial gas saturation in tight sandstones. *J. Geophys. Res.* **89**, 11549–11559.

Nur, A., & Simmons, G., 1969, The effect of saturation on velocity in low porosity rocks. *Earth and Planet. Sci. Lett.* **7**, 183–193.

Ostrander, W. J., 1984, Plane-wave reflection coefficients for gas sands at non-normal angles of incidence: *Geophysics* **49**, 1637–1648.

Wyllie, M. R. J., Gregory, A. R., & Gardner, L. W., 1956, Elastic wave velocities in heterogeneous and porous media: *Geophysics*, **21**, 41–70.

Wyllie, M. R. J., Gregory, A. R., & Gardner, G. H. F., 1958, An experimental investigation of factors affecting elastic wave velocities in porous media: *Geophysics* **23**, 459–493.

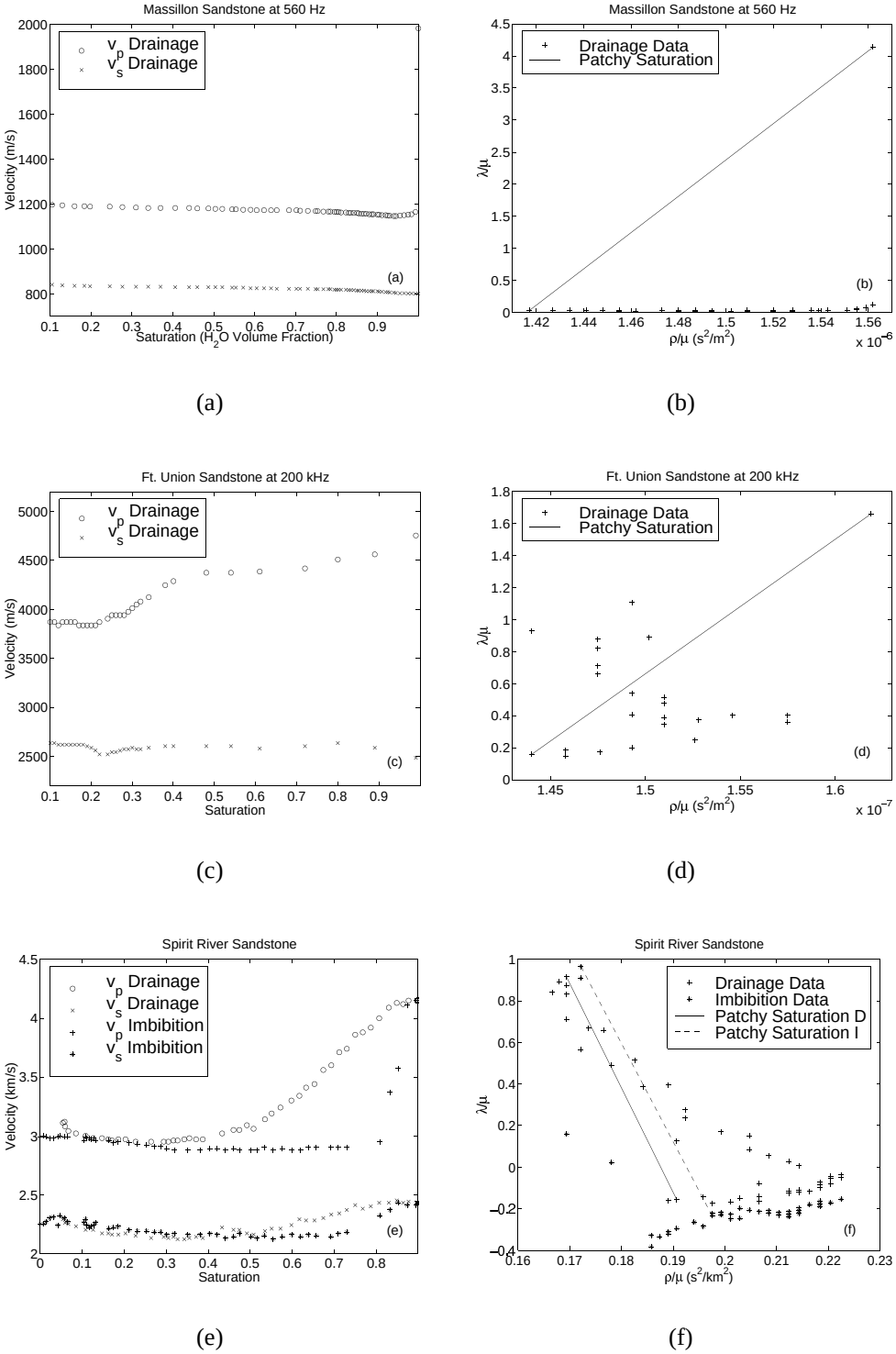

(a) (b)

(c) (d)

(e) (f)

Figure 1: Compressional and shear velocities for Massilon and Ft. Union sandstone measured by Murphy (1982; 1984) and for Spirit River sandstone measured by Knight and Nolen-Hoeksema (1990).

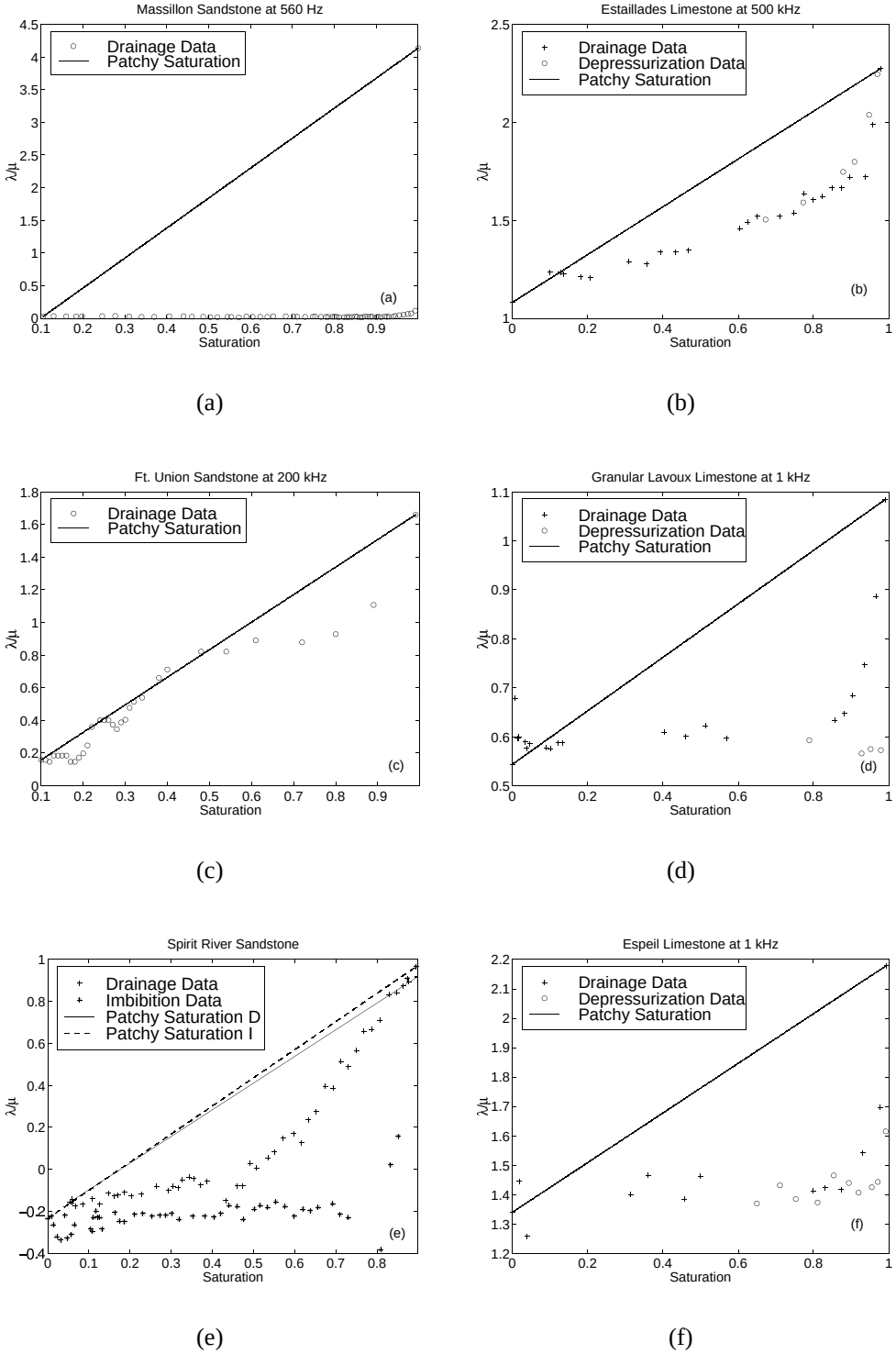

Figure 2: Ratio λ/μ versus saturation for the three sandstones (Murphy, 1982; 1984; Knight and Nolen-Hoeksema, 1990) of Figure 1 and for three limestones (Cadoret, 1993; Cadoret *et al.*, 1995; Cadoret *et al.*, 1998).

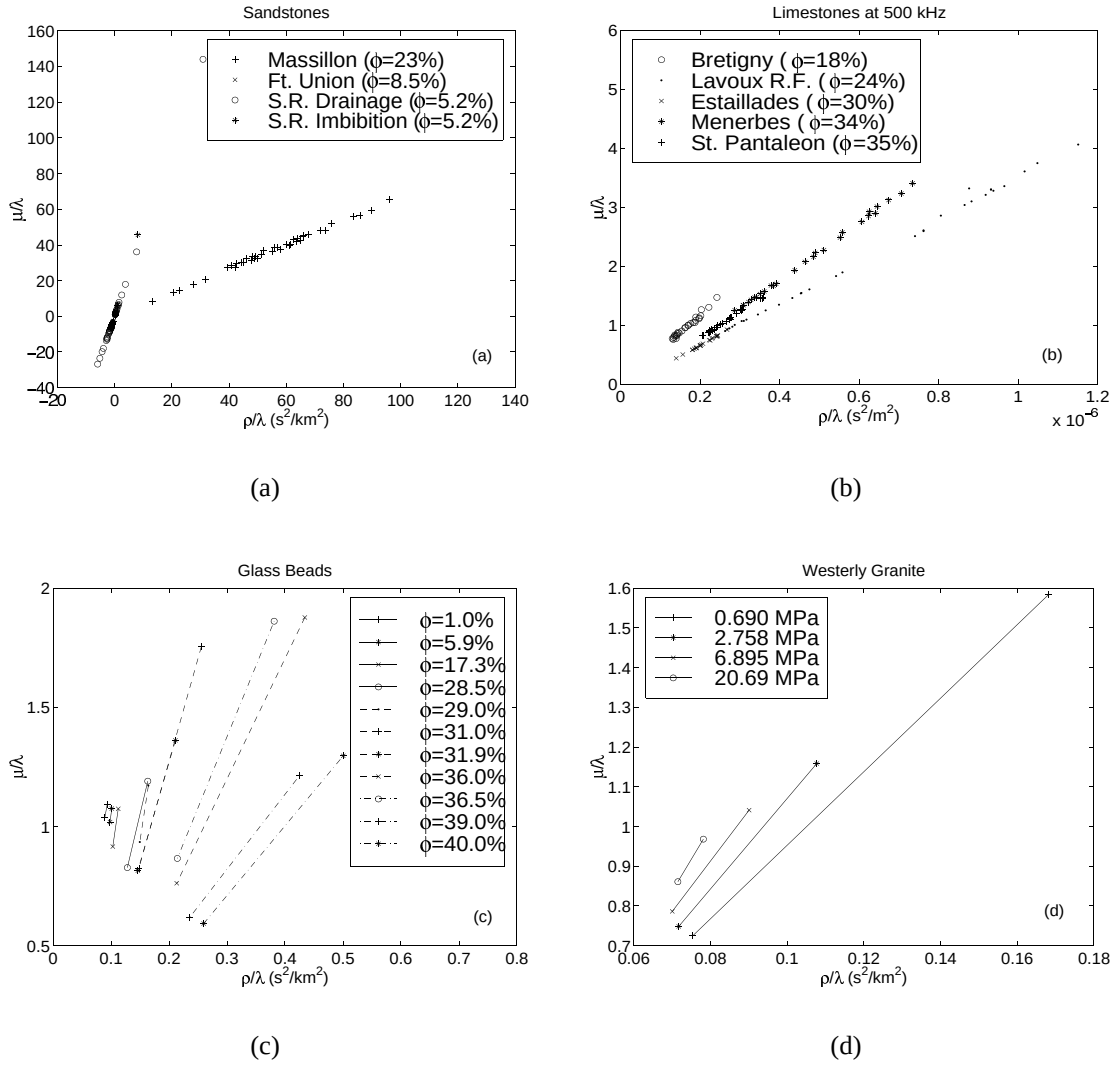

(a) (b)

(c) (d)

Figure 3: Examples of the correlation of slopes with porosity: (a) three sandstones (Murphy, 1982; 1984; Knight and Nolen-Hoeksema, 1990), (b) five limestones (Cadoret, 1993; Cadoret *et al.*, 1995; Cadoret *et al.*, 1998), (c) 11 fused glass-bead samples (Berge *et al.*, 1995), (d) Westerly granite (Nur and Simmons, 1969) at four pressures. The observed trend is that high porosity samples generally have lower slopes than lower porosities on these plots, although there are a few exceptions as discussed in the text. These trends are easily understood since the slopes are determined approximately by the average value of v_s^2 for each material, which is a decreasing function of porosity.